used in this experiment suggests that the low-temperature value of λ_L is larger than that expected for a fully oxygenated sample and hence there is probably a degree of inhomogeneity in the oxygen stoichiometry within the bulk of the crystal. However, the temperature dependence of σ^2, which should be proportional to F^2 for neutron scattering, can be scaled to lie close to the model curve in Fig. 3. Thus there is an intriguing difference between the neutron data and the model curve, but it would be premature to take this as a definite sign of the melting of the flux-line lattice. Nonetheless these experiments clearly demonstrate the potential of neutron scattering as a tool for investigating the local and long-range structure of the magnetic field in the mixed state for high-T_c superconductors. □

Received 3 January; accepted 30 January 1990.

1. Christen, D. K., Kerchner, H. R., Sekula, S. T. & Thorel, P. *Phys. Rev.* B **21,** 102–117 (1980).
2. Brandt, E. H. *Phys. Rev. Lett.* **63,** 1106–1109 (1989).
3. Gammel, P. L., Schneemeyer, L. F., Waszczak, J. V. & Bishop, D. J. *Phys. Rev. Lett.* **61,** 1666–1669 (1988).
4. Kleiman, R. N., Gammel, P. L., Schneemeyer, L. F., Waszczak, J. V. & Bishop, D. J. *Phys. Rev. Lett.* **62,** 2331 (1989).
5. Gammel, P. L. *et al. Phys. Rev. Lett.* **59,** 2592–2595 (1989).
6. Dolan, G. J., Chandrasekhar, G. V., Dinger, T. R., Feild, C. & Holtzberg, F. *Phys. Rev. Lett.* **62,** 827–830 (1989).
7. Forgan, E. M. *Nature* **329,** 483–485 (1987).
8. Pumpin, B. *et al. Physica* C **162–164,** 151–152 (1989).
9. Harshman, D. R. *et al. Phys. Rev.* B **39,** 851–854 (1989).
10. Schelten, J., Lippmann, G. & Ullmaier, H. *J. Low Temp. Phys.* **14,** 213–225 (1974).
11. Christen, D. K., Tasset, F., Spooner, S. & Mook, H. A. *Phys. Rev.* B **15,** 4506–4509 (1977).
12. Ibel, K. *J. appl. Crystallogr.* **9,** 296–308 (1976).

ACKNOWLEDGEMENTS. We thank W. Cheape and R. Baker for technical support, without which this experiment could not have been performed, and M. Moore for encouragement. This work was supported by funding from the NCS and NBRC of the SERC.

Femtosecond laser observations of molecular vibration and rotation

M. Dantus, R. M. Bowman & A. H. Zewail

Arthur Amos Noyes Laboratory of Chemical Physics,
California Institute of Technology, Pasadena, California 91125, USA

ULTRAFAST molecular vibrations and rotations are the fundamental motions that characterize chemical bonding and determine reaction dynamics at the molecular level. The timescales for these motions are typically 10^{-13} s for vibrations and 10^{-10} s for rotations. For decades, time-integrated (frequency-resolved) spectroscopy has provided a powerful tool for probing the dynamics of motion, but the motions themselves are not 'seen' directly in real-time. With femtosecond laser techniques[1–4] it is now possible to follow the motions of isolated molecular systems as they occur. The requirement is that the system is excited (for vibration) and aligned (for rotation) on a timescale shorter than the vibrational and rotational periods. Here we report real-time observations of these molecular motions. The system—in this case, molecular iodine—is prepared in the particular state(s) of interest by coherent excitation with an initial femtosecond laser pulse, and the subsequent motions are probed with successive femtosecond pulses. The probe monitors changes in the interatomic distance (vibration) or molecular orientation (rotation), so that the measured signal provides direct 'snapshots' of the molecular motions.

Figure 1 illustrates the fundamental motions for simple vibrating (harmonic) and rotating diatomic molecules. The vibrational motion (Fig. 1*a*) describes the change in interatomic distance, R, which is characterized by the natural frequency, ν, of the oscillator. The real-time rotational motion of a molecular ensemble (Fig. 1*b*) can be understood by considering the following simple motion of, say, three rotors. At time $t = 0$, the rotors are aligned in the same direction. As time passes, the molecules rotate at different angular velocities (depending on the angular-momentum quantum number $J = 1, 2, 3$) and the initial alignment is lost. At $t = 1/(8B)$ and $3/(8B)$ (where B is the rotational constant of the diatomics), the degree of alignment of the molecules is at a minimum. At $t = 1/(2B)$, all the molecules have performed an integral number of rotations, so that there is a recurrence of the alignment. Thus the full rotational period of the motion is $1/(2B)$. To observe these motions in real-time, the probe must be sensitive to changes in R (for vibration) and in alignment (for rotation).

Femtosecond transition-state spectroscopy (FTS) is our tool for these experiments. In previous FTS studies[5–8] of chemical reactions, the transition-state region between reagents and products was probed. When studying molecular motions of a bound state, there exists, of course, no transition state in the conventional sense; but one is still monitoring transitory changes of R and alignment, so that FTS can be generalized to investigate bound as well as unbound states. The technique uses two femtosecond pulses of different wavelengths and known relative polarizations. The first ('pump') pulse (λ_1 in Fig. 1*c*), which establishes the zero of time, excites the iodine molecules to the bound B state. This event prepares an ensemble of molecules coherently in one (or more) vibrational states, fixing the starting point of the oscillatory motion. Subsequent interrogation is carried out at successive (clocked) time delays by the second femtosecond laser pulse (λ_2^* in Fig. 1*c*).

As the molecule vibrates, the internuclear separation of the iodine atoms changes. At a certain point along the vibrational coordinate R, the probe light is absorbed and the molecule is excited to a specific vibrational level in an upper electronic state, which is determined by the Franck–Condon principle. This upper electronic state is fluorescent, and we monitor this laser-induced fluorescence (LIF) as a function of the time delay between the pump and probe pulses. Thus, as the atoms depart from and return to their initial positions over one vibrational period, the LIF signal varies accordingly, and we obtain a record of how R varies with time. If the vibrational motion is harmonic, only one frequency of oscillation will be observed (see Fig. 1*a*). For anharmonic vibration, on the other hand, the frequency of oscillation depends on the energy. This would result in a simultaneous excitation of a superposition of these frequencies (that is, a wave packet), as shown in Fig. 2.

To observe molecular rotations in real-time, it is necessary to establish more than just the zero of time. The pump pulse must excite the ensemble of molecules so that the subsequent rotational evolution can be followed as illustrated in Fig. 1*b*. To do this we use a polarized laser pulse[9–10] to prepare the iodine molecules coherently in different rotational (J) levels. Only those molecules that have their transition moment $\boldsymbol{\mu}$ (which is parallel to the internuclear axis) parallel or nearly parallel to the polarization plane of the electric field, $\mathbf{E}$, are excited, because the transition amplitude is determined by $\boldsymbol{\mu} \cdot \mathbf{E}$. This anisotropic excitation of the ensemble establishes the initial alignment. The polarized femtosecond probe pulse can be fixed either parallel or perpendicular to these initially aligned iodine molecules. As the probing light is sensitive to the same transition moment (that is, both the pump and probe processes are parallel transitions), the LIF signal at early times (when very little rotation has taken place) will be large for the parallel case and small for the perpendicular one. This is illustrated in Fig. 1*b* and can be seen very clearly in the experimental results of Fig. 3*a*. As the rotation of the ensemble evolves, higher J levels rotate more quickly than lower J levels and the coherence decays. The broader the distribution of rotational levels accessed by the pump pulse, the faster this coherence disappears through dephasing of the alignment[11,12].

The iodine molecules are isolated and freely rotating, so a rephasing of the alignment (a rotational recurrence) should be seen at later times. The recurrence time is determined solely (if we ignore centrifugal distortion) by the rotational constant, B,

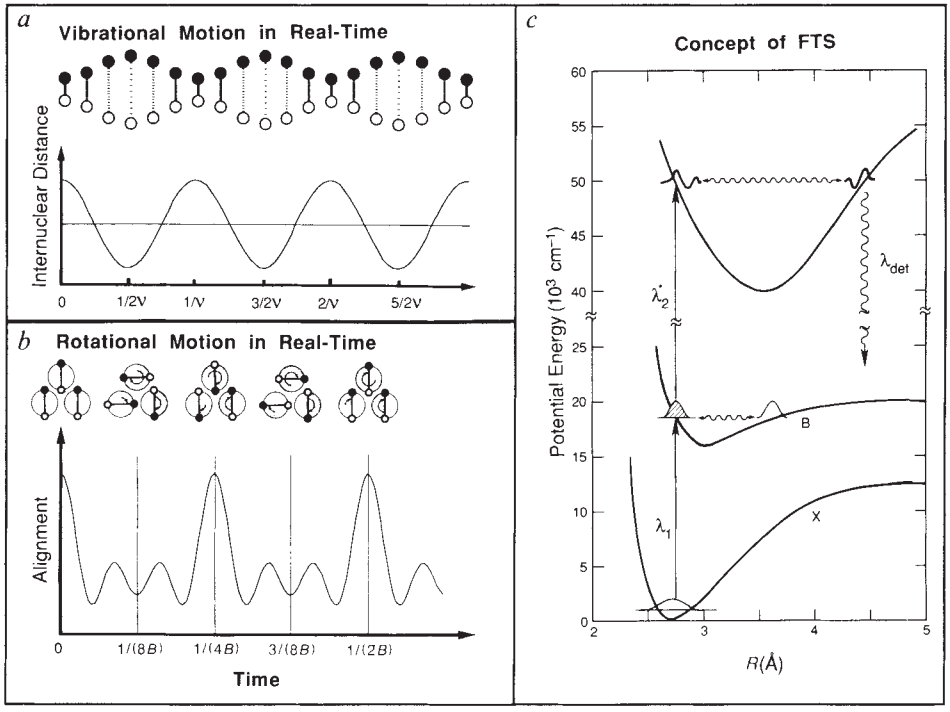

FIG. 1 *a*, Single vibrational (harmonic) motion, with the expected change, in real-time, of the internuclear distance, *R*. The peaks and valleys correspond to a fully compressed and fully extended bond, respectively. *b*, Molecular rotation for an ensemble of three idealized rotors, showing the initial dephasing and the half and full recurrence of the alignment at later times (see text). It should be noted that a quantum-mechanical picture[11,12] of rotations predicts that the half recurrence at $1/(4B)$ is 180° out of phase (negative signal). The shaded region of the circles denotes the amount of rotation that the molecules have executed for each time step. The atoms are shown as black or white for clarity. *c*, Energy-level diagram for FTS. The first femtosecond laser pulse (λ_1) excites the iodine molecules to the B $^3\Pi_{0^+u}$ state, with accompanying vibrational and rotational excitation. The probing is carried out by a second femtosecond laser pulse (λ_2^*), which takes them to the upper fluorescent state. The signal detected (λ_{det}) is fluorescence from the upper electronic state. Absorption or ionization at λ_2^* can also be used.

of the particular vibrational level accessed, being given by $1/(2B)$. Therefore, a rotational recurrence will be seen for each vibrational level accessed; in Fig. 1*b* the result is shown when only a single vibrational level is excited, whereas experimentally (Fig. 3) several are accessed. The spacing between the rotational recurrences is determined by the difference in the values of *B* for each vibrational level involved. Thus, rotational motions are manifested in two ways: an early-time dephasing owing to the initial loss of alignment and a longer-time recurrence owing to rephasing of this alignment.

In Fig. 2*a* we show vibrational transients obtained by exciting iodine molecules at room temperature into the B state using a 620-nm pump beam and probing at 310 nm. The transients are free from rotational effects, which is achieved by orientating the probe polarization at the magic angle (54.7°) with respect to the pump[11,12]. The most striking feature of this figure is the fast oscillations with a period of 300 fs; this corresponds to the vibrational period. Their amplitude is modulated with a much longer period of 10 ps. This behaviour is due to the anharmonicity of the vibration, manifested by the interferences of the different vibrational frequencies in the wave packet.

Direct comparisons can be made with these real-time experiments, because the high-resolution spectroscopy of iodine has been studied extensively[13–16]. Femtosecond excitation at 620 nm

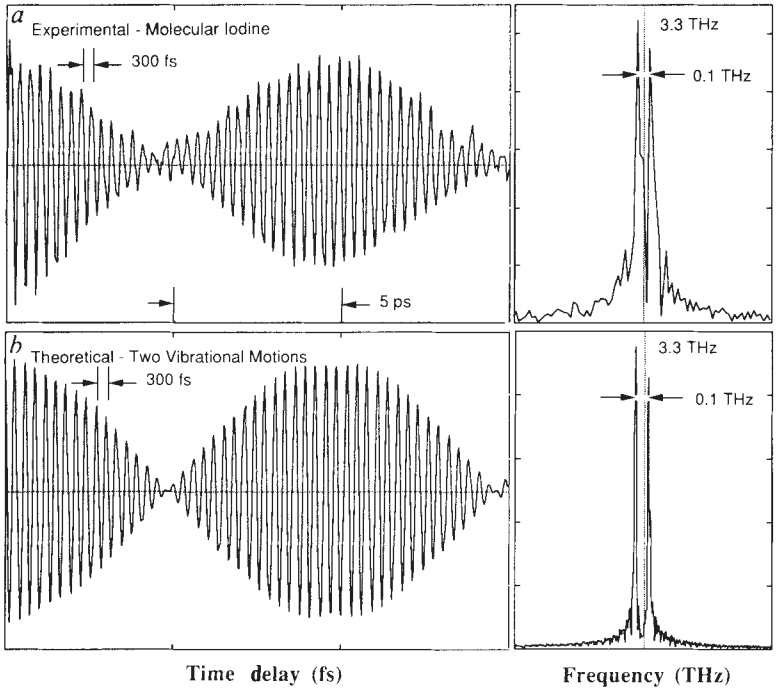

FIG. 2 *a*, FTS transients showing real-time vibrations of molecular iodine (left). The vertical scale represents the LIF amplitude, which is a probe of the internuclear distance. The corresponding Fourier transform is shown on the right. *b*, Calculated results for excitation of a wave packet comprising the two principal vibrational frequencies in *a*, and the corresponding Fourier transform.

should access vibrational levels 7 to 12; because of anharmonicity, the vibrational frequencies of these levels differ slightly and the average frequency should be 3.3 THz (refs 13–16), which is in excellent agreement with our results. The Fourier transform of the rotation-free transient is also shown in Fig. 2*a* and is consistent with the analysis above. Closer inspection of the transform reveals several peaks, corresponding to the several vibrational levels excited. The frequencies of the two largest peaks were used to simulate the transient (Fig. 2*b*). The complete transform has been used to obtain the potential-energy surface governing the motion of the two iodine atoms, and this analysis will be published elsewhere (M.D., R.M.B., A.H.Z., M. Gruebele and G. Roberts, manuscript in preparation). In Fig. 3 we show the results obtained for rotational motion. These were obtained under conditions identical to those of Fig. 2 except that the relative polarizations of the pump and probe pulses were fixed to be either parallel or perpendicular, so as to monitor the alignment. The initial loss of alignment is seen clearly in the early-time behaviour of the parallel and perpendicular transients. The amplitudes, initially different, approach a constant value within the first 3 ps. At much longer times (~600 ps), rotational recurrences are seen for each of the six vibrational levels accessed. The vibrational and rotational motions are clearly separable in time, because their periods (~300 fs and ~600 ps respectively) differ by three orders of magnitude. The fact that each vibration gives rise to a rotational recurrence (as in Fig. 3) means that rotational constants can be obtained for each vibrational level. A calculation of the expected results, taking into account the known rotational constants[13–16] and the centrifugal distortion[13–16] (that is, the changes in the equilibrium bond distance resulting from rotation), for the vibrational levels 7 to 12, is shown in Fig. 3*b*. The agreement with experiment is excellent. Finally, theory[11,12] predicts that parallel and perpendicular recurrences should be 180° out of phase and that a half recurrence at $1/(4B)$ should occur. The former effect is seen in Fig. 3*a* and the latter has been observed (not shown in Fig. 3); both are in accord with theory.

The FTS experiments reported here provide direct observations of the vibrational and rotational motions in isolated molecular systems. The method allows the quantum-mechanical wave-packet dynamics to be studied in real-time and related to the molecular potential-energy surface. In the early stages of FTS, the focus was on reactive processes (bond breaking or forming), but this time-resolved spectroscopy can now be applied to bound molecular systems. □

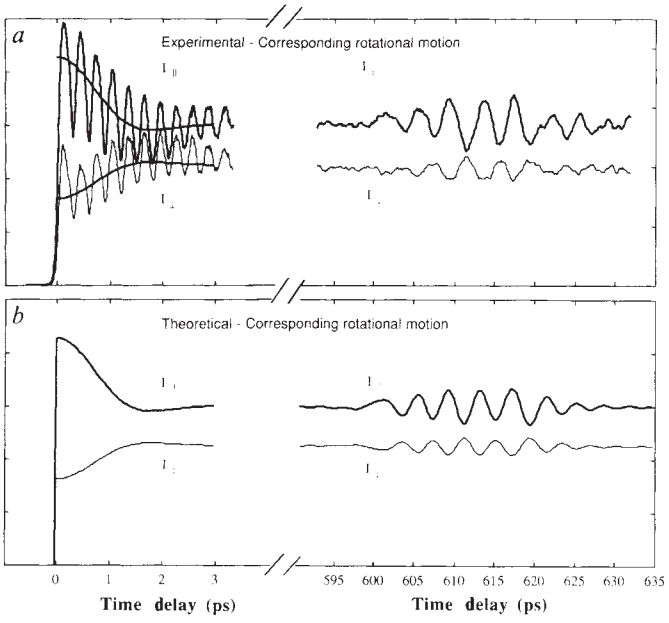

FIG. 3 Polarized FTS of molecular iodine. *a*, Transients showing the initial dephasing owing to molecular rotation (left) and the appearance of full recurrences at a later time (right). Parallel and perpendicular probe orientations are shown (see text), and are 180° out of phase, as expected. The rapid oscillations are due to vibrational excitation; six levels are accessed (the solid line through these on the left is a guide to the eye). Half recurrences were observed experimentally, but are not shown here. Note that the time scale is discontinuous. *b*, Calculated results for rotational dephasing (left) and rephasing (right), assuming excitation of vibrational levels 7 to 12 and taking into account vibrational and rotational coupling and centrifugal distortion.

Received 19 December 1989; accepted 25 January 1990.

1. Zewail, A. H. *Science* **242,** 1645–1653 (1988).
2. Zewail, A. H. & Bernstein, R. B. *Chem. Engng News* **66,** 24–43 (1988).
3. Smith, I. W. M. *Nature* **328,** 760–761 (1987).
4. Baggot, J. *New Scientist* **1669,** 58–62 (1989).
5. Dantus, M., Rosker, M. J. & Zewail, A. H. *J. chem. Phys.* **89,** 6128–6140 (1988).
6. Bowman, R. M., Dantus, M. & Zewail, A. H. *Chem. Phys. Lett.* **161,** 297–302 (1989).
7. Rose, T. S., Rosker, M. J. & Zewail, A. H. *J. chem. Phys.* **91,** 7415–7436 (1989).
8. Dantus, M., Bowman, R. M., Gruebele, M. & Zewail, A. H. *J. chem. Phys.* **91,** 7437–7450 (1989).
9. Zewail, A. H. *J. chem. Soc. Faraday Trans. II* **85,** 1221–1242 (1989).
10. Dantus, M., Bowman, R. M., Baskin, J. S. & Zewail, A. H. *Chem. Phys. Lett.* **159,** 406–412 (1989).
11. Felker, P. M. & Zewail, A. H. *J. chem. Phys.* **86,** 2460–2482 (1987).
12. Baskin, J. S., Felker, P. M. & Zewail, A. H. *J. chem. Phys.* **86,** 2483–2499 (1987).
13. Mulliken, R. S. *J. chem. Phys.* **55,** 288–309 (1971).
14. Tellinghuisen, J. *J. chem. Phys.* **58,** 2821–2834 (1973).
15. Gerstenkorn, S. & Luc, P. *J. Phys. (Paris)* **46,** 867–881 (1985).
16. Brand, J. C. D. & Hoy, A. R. *Appl. Spectrosc. Rev.* **23,** 285–327 (1987).

ACKNOWLEDGEMENTS. This work was supported by the NSF.

Polyethylene oxide does not necessarily aggregate in water

K. Devanand & J. C. Selser

Department of Physics, University of Nevada at Las Vegas, Las Vegas, Nevada 89154, USA

POLYETHYLENE oxide (PEO) is one of the most extensively studied of all water-soluble synthetic polymers, both for its wide range of applications[1–4] and from the fundamental standpoint of understanding the behaviour of polymer solutions. The aggregation behaviour of PEO in water and its consequences have been a matter of concern in many studies[5–11] of this system. It is not clear, however, whether PEO aggregation is an inherent property of these aqueous solutions, although this knowledge can have important and widespread consequences for both industry and polymer science. Here we use dynamic light scattering from high-molecular-weight PEO in carefully purified water and in methanol to show unambiguously that both are good solvents in the sense that PEO behaves like a typical random coil in both, with no evidence of aggregation.

The hypothesis that aggregation is an inherent property of PEO/water systems has been supported both by electron microscopy investigations[9] and by the observation of time-dependent PEO aggregrates in aqueous solutions of the polymer on the basis of light-scattering studies[10]. This is in contrast to the use of methanol as the solvent—methanol is known to be a dispersing solvent for PEO[11,12]. Furthermore, discrepancies in solvent quality, as recorded by differences in the value of the exponent a in the relation between molecular weight (M) and intrinsic viscosity (η), $[\eta] \propto M^a$, have been ascribed to aggregration of the polymer in water[13]. To clarify these issues and to test the 'aggregation hypothesis', we have carried out parallel dynamic light-scattering measurements of linear polyethylene oxide both in methanol and in water.

Dynamic light scattering is a non-invasive and accurate technique for the measurement of the diffusion coefficient D of